Published in final edited form as:
Nanomedicine. 2015 February ; 11(2): 401–405. doi:10.1016/j.nano.2014.09.019.

Liposome-based mucus-penetrating particles (MPP) for mucosal theranostics: Demonstration of diamagnetic chemical exchange saturation transfer (diaCEST) magnetic resonance imaging (MRI)

Tao Yu, BS[a,f,1], **Kannie W. Y. Chan, PhD**[d,f,1], **Abraham Anonuevo**[b,f], **Xiaolei Song, PhD**[d,e], **Benjamin S. Schuster, BS**[a,f], **Sumon Chattopadhyay, MS**[b,f], **Qingguo Xu, PhD**[c,f], **Nikita Oskolkov, PhD**[d,e], **Himatkumar Patel, PhD**[c,f], **Laura M. Ensign, PhD**[c,f], **Peter C. M. van Zjil, PhD**[d,e], **Michael T. McMahon, PhD**[*,d,e,f], and **Justin Hanes, PhD**[*,a,b,c,f]

[a]Department of Biomedical Engineering, Johns Hopkins University School of Medicine, 720 Rutland Avenue, Baltimore, MD 21205 (USA)

[b]Department of Chemical and Biomolecular Engineering, Johns Hopkins University, 3400 N Charles Street, Baltimore, MD 21218 (USA)

[c]Department of Ophthalmology, The Wilmer Eye Institute, Johns Hopkins University School of Medicine, 400 N Broadway, Baltimore, MD 21287 (USA)

[d]Russell H. Morgan Department of Radiology and Radiological Sciences, Division of MR Research, The Johns Hopkins University School of Medicine, Baltimore 21287, USA

[e]F.M. Kirby Research Center for Functional Brain Imaging, Kennedy Krieger Institute, Baltimore 21205, USA

[f]Center for Nanomedicine, Johns Hopkins University School of Medicine, 400 N Broadway, Baltimore, MD 21231 (USA)

Abstract

Mucus barriers lining mucosal epithelia reduce the effectiveness of nanocarrier-based mucosal drug delivery and imaging (“theranostics”). Here, we describe liposome-based mucus-penetrating particles (MPP) capable of loading hydrophilic agents, e.g., the diaCEST MRI contrast agent barbituric acid (BA). We observed that polyethylene glycol (PEG)-coated liposomes containing ≥7 mol% PEG diffused only ~10-fold slower in human cervicovaginal mucus (CVM) compared to

[*]Corresponding authors: Justin Hanes, Ph.D., The Center for Nanomedicine, Johns Hopkins University School of Medicine, 400 N Broadway, Baltimore, MD 21231 (USA), Tel: + 1-410-614-6513, Fax: + 1-443-287-7922, hanes@jhu.edu, Michael T. McMahon, Ph.D., F.M. Kirby Research Center for Functional Brain Imaging, Kennedy Krieger Institute, 707 N Broadway, Baltimore, MD 21205 (USA), mtmcmaho@gmail.com.
[1]These authors contributed equally.

Disclosure of conflicts of interest:
The mucus-penetrating particle technology is being developed by Kala Pharmaceuticals. J.H. is co-founder and consultant to Kala and owns company stock, which is subject to certain restrictions under Johns Hopkins University policy. The terms of this arrangement are being managed by the Johns Hopkins University in accordance with its conflict of interest policies.

their theoretical speeds in water. 7 mol%-PEG liposomes contained sufficient BA loading for diaCEST contrast, and provided improved vaginal distribution compared to 0 and 3 mol%-PEG liposomes. However, increasing PEG content to ~12 mol% compromised BA loading and vaginal distribution, suggesting that PEG content must be optimized to maintain drug loading and *in vivo* stability. Non-invasive diaCEST MRI illustrated uniform vaginal coverage and longer retention of BA-loaded 7 mol %-PEG liposomes compared to unencapsulated BA. Liposomal MPP with optimized PEG content hold promise for drug delivery and imaging at mucosal surfaces.

Keywords

drug and gene delivery; lipid; CEST; barbituric acid

Background

Mucosal drug delivery via nano-carriers holds potential to improve detection and treatment of numerous diseases.[1, 2] For efficient mucosal delivery, nano-carriers must first bypass the highly protective mucus linings that rapidly remove most foreign particles from the mucosae.[3] To overcome the mucus barrier, we have previously developed polymer- and pure drug-based nanoparticulates that possess dense coatings with polyethylene glycol (PEG) that effectively avoid mucoadhesion, thus allowing rapid penetration through mucus.[4] As a result, these mucus-penetrating particles (MPP) provide more uniform distribution and sustained delivery of therapeutics at various mucosal sites.[5–7]

Liposomes were the first nano-carrier system to be developed and translated for clinical use.[8] Although liposomal systems have been explored for mucosal delivery,[9, 10] there has not been a focus on directly observing the interactions of liposomal formulations with mucus, and how these interactions impact mucosal distribution. Here, we varied the composition of PEG-conjugated lipids to investigate the effect of PEG surface density on liposome mobility in human cervicovaginal mucus (CVM) and vaginal distribution *in vivo*. Chemical Exchange Saturation Transfer (CEST) Magnetic Resonance Imaging (MRI) contrast agents have shown great promise, particularly due to their capability of being distinguished from each other through artificial color contrast.[11] As a demonstration, we loaded the liposomal MPP with barbituric acid (BA), a water-soluble, highly biocompatiblediamagnetic CEST (diaCEST) contrast agent,[12] and monitored the vaginal distribution and retention of the liposomes via MRI.[11, 13]

Methods

Liposomes composed of 1,2-disteoroyl-*sn*-glycero-3-phosphatidylcholine (DSPC), cholesterol, and 1,2-distearoyl-*sn*-glycerophosphoethanolamine poly(ethylene glycol)$_{2000}$ (DSPE-PEG$_{2k}$) were prepared and characterized following procedures adapted from previous reports.[5, 12, 14, 15] Human CVM was collected following a protocol approved by the Johns Hopkins School of Medicine Institutional Review Board; all patients provided written informed consent. All animal studies were performed in accordance to protocols approved by the Institutional Animal Care and Use Committee (IACUC) at the Johns Hopkins University; humane care of all animals used in the studies was provided. Full

methods, including liposome tracking in mucus, animal studies, and MRI protocols, are provided in Supporting Information. Data represent mean ± standard error of the mean (S.E.M.).

Results

We first formulated DSPC liposomes containing 6 different ratios of DSPE-PEG_{2k} (Table 1). We used extrusion to reduce the mean diameters of all formulations to below the average mesh size of human CVM (~340 nm)[4] to minimize steric hindrance. The PEGylated formulations were relatively uniform in size (low polydispersity index, or PDI), whereas non-PEGylated liposomes displayed high PDI, implying aggregation occurred. We also measured the actual molar fraction of DSPE-PEG_{2k} and estimated the PEG surface density. The Γ/SA ratios (theoretical area covered by unconstrained PEG chains vs. total surface area of a liposome,[14] see Supporting Information) suggest that liposomes with ≥ 7 mol%-PEG were coated with brush-like PEG chains forming effective surface shielding, whereas those with ≤ 5 mol%-PEG were covered with mushroom-like PEG chains and, thus, less effectively shielded.[14]

We then investigated the diffusion of liposomes immediately (0 h) and 3 h after addition to CVM via multiple particle tracking (MPT).[15] PEGylated liposomes diffused overall faster than the non-PEGylated liposomes, exhibiting more diffusive trajectories and ~10-fold higher ensemble-averaged mean-squared displacement (<MSD>) (Figure 1, A-B). A significant population of immobilized non-PEGylated liposomes was revealed in the logarithmic distribution of individual liposome MSD (Figure 1, C). The <MSD> of PEGylated and non-PEGylated liposomes was ~10- and 110-fold slower than their theoretical MSD in water (t = 1 s), respectively (Table 1). After 3 h incubation in CVM, liposomes with lower PEG content (0 – 5 mol%) displayed more restricted trajectories and ~2-fold decrease in <MSD>, with an increased immobilized fraction (Figure 1, A-C). Overall, liposomes with ≥ 7 mol% PEG diffused similarly in CVM compared to polymeric MPP ($MSD_w/<MSD>_m$ ~10)[5, 14] and the mobility remained stable over time. Next, we prepared BA-loaded liposomes for diaCEST MRI (Table 2). BA encapsulation minimally affected the liposome size and PDI. The loading capacity (BA:lipid ratio) correlated inversely with PEG content, with a substantial decrease at 12 mol%-PEG, likely due to reduced free volume associated with high PEG content on the inner surface of the liposomal shell, and the increased permeability of the lipid bilayer.[16] The *in vitro* CEST contrast was generally consistent with the BA loading level.

We next investigated the vaginal distribution of BA-loaded liposomes in the vaginas of mice in the estrus phase of their estrous cycle.[5] Particle mobility in mucus has been demonstrated to correlate with *in vivo* mucosal distribution.[5–7] Similarly, we observed non-uniform distribution of mucoadhesive, non-PEGylated liposomes, which appeared to outline mucin bundles (Figure 2, A). This non-uniform distribution was also reflected by a high variance-to-mean ratio (VMR, increased VMR reflects decreased uniformity) (Figure 2, E). While all PEGylated liposomes provided improved vaginal distribution, 7 mol%-PEG liposomes demonstrated the most uniform coverage with the lowest VMR. Additionally, individual cell outlines were observed, implying that the 7 mol%-PEG liposomes were able to reach the

vaginal epithelium (Figure 2, C). Liposomes with less PEG content may be insufficiently shielded to avoid mucoadhesion *in vivo*. Despite rapid diffusion in CVM, the 12 mol%-PEG liposomes also distributed suboptimally *in vivo* (Figure 2, D), perhaps due to their disassembly via micellization *in vivo*.[17] Therefore, PEG content must be optimized to eliminate mucoadhesion while maintaining stability *in vivo*.

Finally, we monitored the vaginal retention of BA-loaded liposomes via diaCEST MRI. 7 mol%-PEG liposomes were selected as liposomal MPP given their sufficient loading and retention of BA (Figure S1) and most uniform vaginal distribution. Liposomal MPP displayed good vaginal coverage with prolonged CEST contrast (at least 90min; highest relative MTR_{asym}^{5ppm}~4%); much shorter vaginal retention time was observed for unencapsulated BA (~30 min; highest relative MTR_{asym}^{5ppm} ~1%) (Figure 3, A-B). The increase in CEST contrast over time for liposomal MPP was likely due to initial spreading throughout the vaginal tract, followed by liposome concentration at the epithelial surface as fluid was absorbed by the epithelium (Figure 3, B). At 90 min, images of liposomal MPP exhibited a significant fraction of high contrast pixels (MTR_{asym}^{5ppm}~5%) (Figure 3, C).

Discussion

The <MSD> of non-PEGylated liposomes in CVM was slightly higher than that of the mucoadhesive polystyrene nanoparticles,[5] implying that the zwitterionic DSPC headgroups may have reduced adhesive (hydrophobic, electrostatic, etc.) interactions with mucus.[4] Nevertheless, adhesion of the liposomes to mucus was apparent, and aggregation of non-PEGylated liposomes may have resulted in further immobilization. PEG-shielding was required to allow effective mucus-penetration; this need for PEG-shielding would likely be higher for liposomes composed of more mucoadhesive lipids, e.g., comprising non-neutral headgroups, such as cationic lipids commonly used for nucleic acid delivery. The gradually decreased mobility of insufficiently PEGylated liposomes in CVM may also result from dissociation of PEGylated lipids over time.

CEST MRI has been previously used to monitor liposomes administered intratumorally and systemically,[12, 18] and here we demonstrate the capability of diaCEST MRI for non-invasive monitoring of liposomes administered intravaginally. Different liposome formulations could also be loaded with CEST agents having distinct chemical shifts, thereby allowing simultaneous monitoring for direct comparison and evaluation of interactions between the formulations.[11] Additionally, diaCEST liposomal MPP may be co-loaded with therapeutics via carefully designed schemes for treatment.[12] These capabilities could enable clinical evaluation of nanocarrier based vaginal therapies, especially when combined with new imaging methods.[19, 20]

In summary, we developed liposomal MPP with optimized surface PEG shielding and capable of loading hydrophilic agents like BA. PEGylation, particularly at levels ≥ 7 mol%, enhanced the mobility of liposomes in human CVM. However, increasing PEGylation to ~12 mol% compromised drug encapsulation and *in vivo* distribution. Moderately PEGylated liposomes (~7 mol%) maintained encapsulation efficiency while distributing most uniformly in the mouse vagina. Using non-invasive diaCEST MRI, we showed that liposomal MPP

provided uniform vaginal coverage and retained BA for ≥ 90 min *in vivo*. These results demonstrate the potential of liposomal MPP for mucosal delivery and imaging, and suggest that liposomal MPP formulations may be suitable for theranostics in mucosal surfaces, like that of the vagina.

Supplementary Material

Refer to Web version on PubMed Central for supplementary material.

Acknowledgements

We thank Ming Yang for helpful discussions and Joshua Kays for technical assistance.

Statements of Funding:

This work was supported in part by NIH grants R01EB015031, R01EB015032, and S10RR028955. The content is solely the responsibility of the authors and does not necessarily represent the official views of the National Institute of Health.

Abbreviations

BA	barbituric acid
CVM	cervicovaginal mucus
diaCEST	diamagnetic chemical exchange saturation transfer
MPP	mucus-penetrating particles
MPT	multiple particle tracking
MRI	magnetic resonance imaging
PEG	polyethylene glycol
DSPC	1,2-disteoroyl-*sn*-glycero-3-phosphatidylcholine
DSPE-PEG$_{2k}$	1,2-distearoyl-*sn*-glycerophosphoethanolamine poly(ethylene glycol)$_{2000}$

References

1. Csaba N, Garcia-Fuentes M, Alonso MJ. The performance of nanocarriers for transmucosal drug delivery. Expert Opin Drug Deliv. 2006; 3:463–478. [PubMed: 16822222]
2. Kammona O, Kiparissides C. Recent advances in nanocarrier-based mucosal delivery of biomolecules. J Control Release. 2012; 161:781–794. [PubMed: 22659331]
3. Laffleur F, Bernkop-Schnurch A. Strategies for improving mucosal drug delivery. Nanomedicine (Lond). 2013; 8:2061–2075. [PubMed: 24279493]
4. Ensign LM, Schneider C, Suk JS, Cone R, Hanes J. Mucus penetrating nanoparticles: biophysical tool and method of drug and gene delivery. Adv Mater. 2012; 24:3887–3894. [PubMed: 22988559]
5. Ensign LM, Tang BC, Wang YY, Tse TA, Hoen T, Cone R, et al. Mucus-penetrating nanoparticles for vaginal drug delivery protect against herpes simplex virus. Sci Transl Med. 2012; 4:138ra79.
6. Yang M, Yu T, Wang YY, Lai SK, Zeng Q, Miao B, et al. Vaginal Delivery of Paclitaxel via Nanoparticles with Non-Mucoadhesive Surfaces Suppresses Cervical Tumor Growth. Adv Healthc Mater. 2014; 3:1044–1052. [PubMed: 24339398]

7. Suk JS, Kim AJ, Trehan K, Schneider CS, Cebotaru L, Woodward OM, et al. Lung gene therapy with highly compacted DNA nanoparticles that overcome the mucus barrier. J Control Release. 2014; 178:8–17. [PubMed: 24440664]
8. Torchilin VP. Recent advances with liposomes as pharmaceutical carriers. Nat Rev Drug Discov. 2005; 4:145–160. [PubMed: 15688077]
9. Li X, Chen D, Le C, Zhu C, Gan Y, Hovgaard L, et al. Novel mucus-penetrating liposomes as a potential oral drug delivery system: preparation, in vitro characterization, and enhanced cellular uptake. Int J Nanomedicine. 2011; 6:3151–3162. [PubMed: 22163166]
10. Wu SY, Chang HI, Burgess M, McMillan NA. Vaginal delivery of siRNA using a novel PEGylated lipoplex-entrapped alginate scaffold system. J Control Release. 2011; 155:418–426. [PubMed: 21315117]
11. Liu G, Song X, Chan KW, McMahon MT. Nuts and bolts of chemical exchange saturation transfer MRI. NMR Biomed. 2013; 26:810–828. [PubMed: 23303716]
12. Chan KW, Yu T, Qiao Y, Liu Q, Yang M, Patel H, et al. A diaCEST MRI approach for monitoring liposomal accumulation in tumors. J Control Release. 2014; 180:51–59. [PubMed: 24548481]
13. Ward KM, Aletras AH, Balaban RS. A new class of contrast agents for MRI based on proton chemical exchange dependent saturation transfer (CEST). J Magn Reson. 2000; 143:79–87. [PubMed: 10698648]
14. Xu Q, Boylan NJ, Cai S, Miao B, Patel H, Hanes J. Scalable method to produce biodegradable nanoparticles that rapidly penetrate human mucus. J Control Release. 2013; 170:279–286. [PubMed: 23751567]
15. Schuster BS, Kim AJ, Kays JC, Kanzawa MM, Guggino WB, Boyle MP, et al. Overcoming the cystic fibrosis sputum barrier to leading adeno-associated virus gene therapy vectors. Mol Ther. 2014; 22:1484–1493. [PubMed: 24869933]
16. Nicholas AR, Scott MJ, Kennedy NI, Jones MN. Effect of grafted polyethylene glycol (PEG) on the size, encapsulation efficiency and permeability of vesicles. Biochim Biophys Acta. 2000; 1463:167–178. [PubMed: 10631306]
17. Garbuzenko O, Barenholz Y, Priev A. Effect of grafted PEG on liposome size and on compressibility and packing of lipid bilayer. Chem Phys Lipids. 2005; 135:117–129. [PubMed: 15921973]
18. Delli Castelli D, Dastru W, Terreno E, Cittadino E, Mainini F, Torres E, et al. In vivo MRI multicontrast kinetic analysis of the uptake and intracellular trafficking of paramagnetically labeled liposomes. J Control Release. 2010; 144:271–279. [PubMed: 20230865]
19. Xu X, Lee JS, Jerschow A. Ultrafast scanning of exchangeable sites by NMR spectroscopy. Angew Chem Int Ed Engl. 2013; 52:8281–8284. [PubMed: 23813633]
20. Dopfert J, Witte C, Schroder L. Slice-selective gradient-encoded CEST spectroscopy for monitoring dynamic parameters and high-throughput sample characterization. J Magn Reson. 2013; 237:34–39. [PubMed: 24135801]

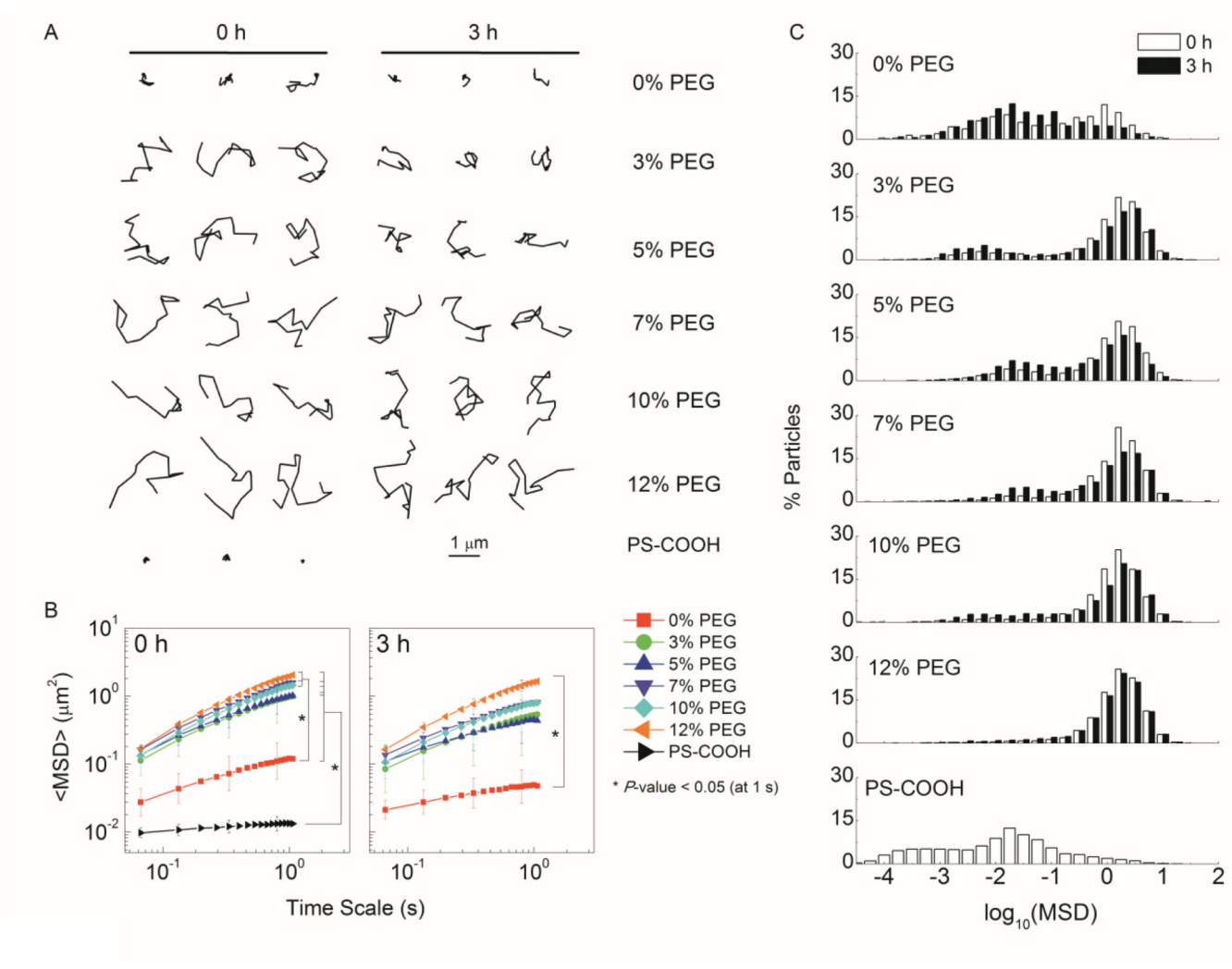

Figure 1.

Mobility of PEGylated and non-PEGylated DSPC liposomes 0 h or 3 h post addition to CVM. **A**. Representative liposome trajectories over 1 s. **B**. <MSD> as a function of time scale. **C**. Distributions of the logarithms of individual liposome MSD.

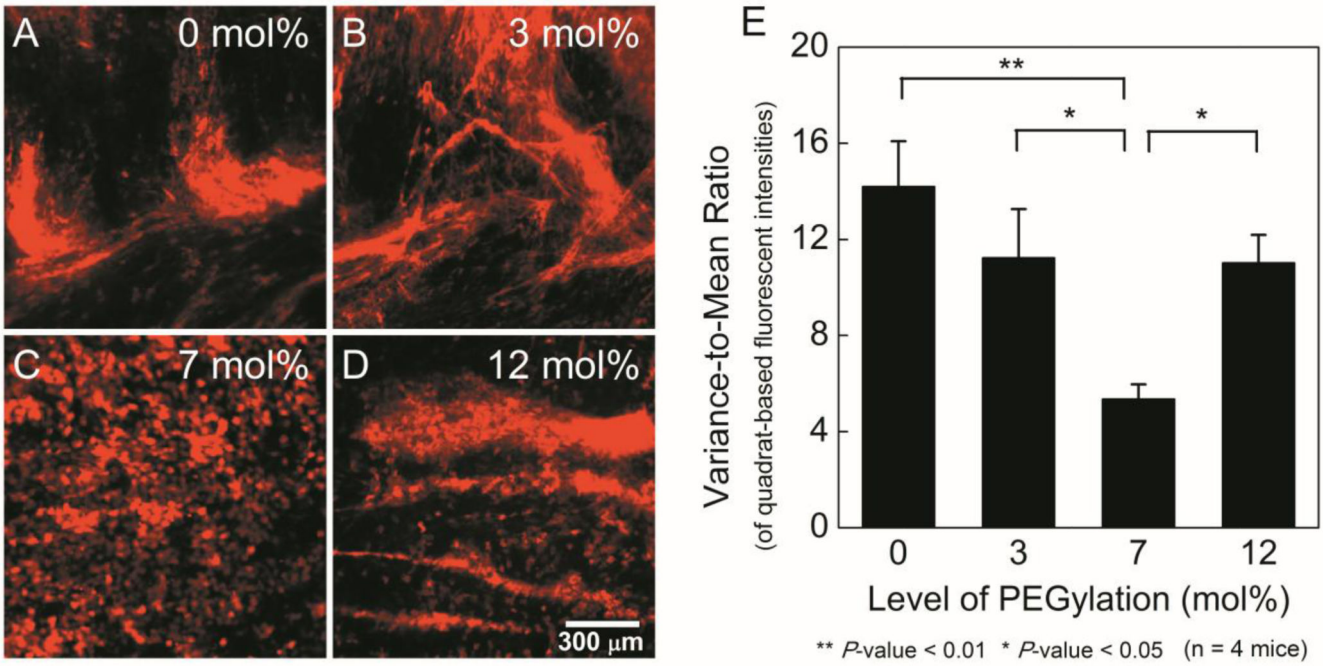

Figure 2.

Distribution of rhodamine-labeled (red) BA-loaded liposomes on flattened mouse vaginal tissues. **A-D**. Representative fluorescence images for different PEGylation levels. **E**. Variance-to-mean ratio of fluorescence intensity (Lower values indicate increased uniformity).

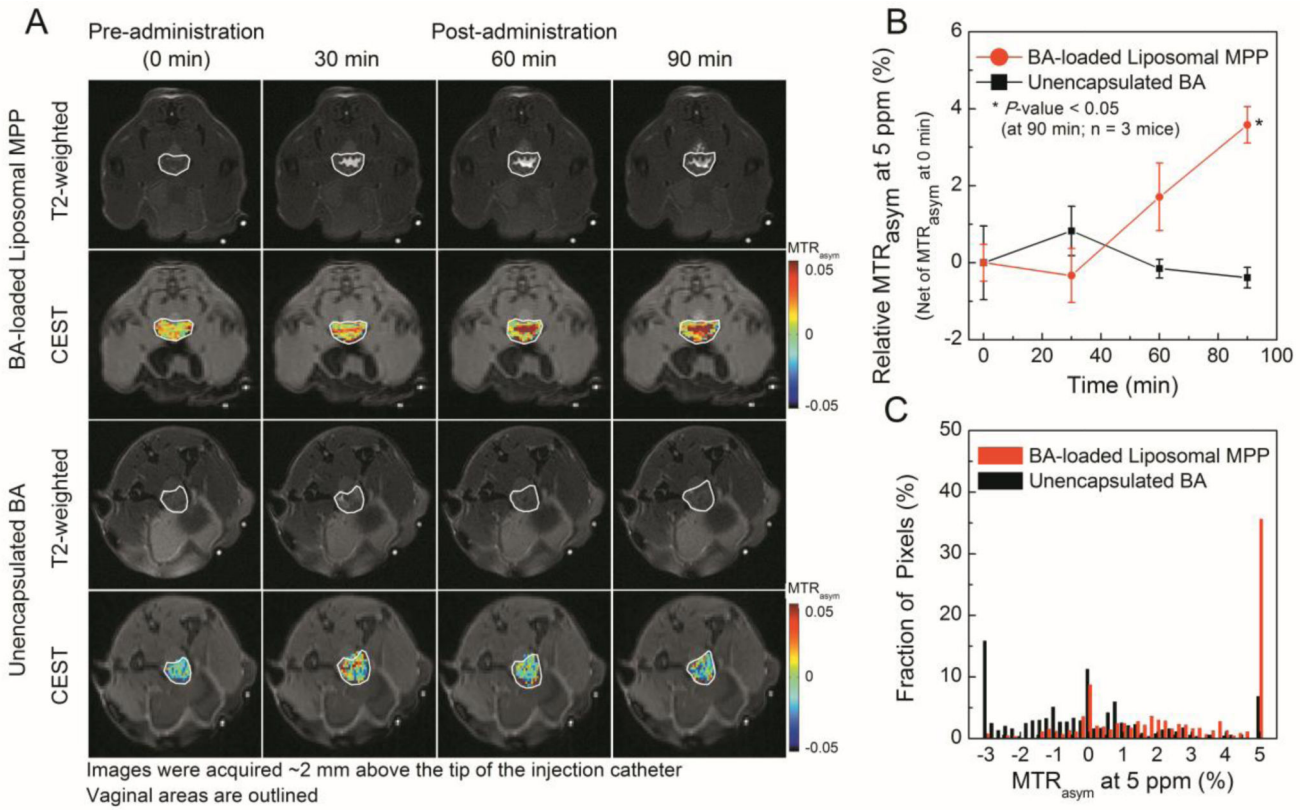

Figure 3.

Monitoring of intravaginally administered BA-loaded liposomal MPP and unencapsulated BA via MRI in mice. **A**. Representative T2-weighted and CEST images. **B**. Relative MTR_{asym} over time. **C**. Histogram of pixelated MTR_{asym} at 90min.

Table 1

Characterization of DSPC liposomes at different PEGylation levels[a]

Sample	Number Mean Diameter (nm)	Polydispersity (PDI)	Actual Mol% of DSPE-PEG_{2k}	PEG Density (Chains/ 100 nm^2)	[Γ/SA][b]	MSDw/<MSD>$_m$[c]	
						0h	3h
0 mol%-PEG	129 ± 18	0.37 ± 0.06	NA	NA	NA	110	270
3 mol%-PEG	134 ± 9	0.09 ± 0.01	3.2 ± 0.1	7.2	0.6	13	25
5 mol%-PEG	121 ± 9	0.06 ± 0.02	4.9 ± 0.1	10.9	0.9	14	31
7 mol%-PEG	139 ± 4	0.06 ± 0.01	6.2 ± 0.1	13.9	1.2	8	15
10 mol%-PEG	147 ± 9	0.03 ± 0.01	8.5 ± 0.2	18.8	1.6	8	15
12 mol%-PEG	149 ± 5	0.04 ± 0.01	10.6 ± 0.3	23.7	2.0	6	7
PS-COOH	91 ± 1	0.04 ± 0.01	NA	NA	NA	1,400	NA

[a] Containing 3-(trimethyl-silyl)-1-propanesulfonic acid sodium salt for NMR measurements.

[b] Ratio of theoretical area covered by unconstrained PEG chains vs. total surface area of a liposome; detailed calculations are provided in Supporting Information.

[b] Ratio of theoretical MSD in water vs. <MSD> measured in CVM; detailed calculations are provided in Supporting Information.

Table 2

Characterization of BA-loaded liposomes

Sample	Number Mean Diameter (nm)	Polydispersity (PDI)	BA:Lipid Ratio (%)	*In vitro* CEST Contrast at 5 ppm (%)
0 mol%-PEG	113 ± 12	0.28 ± 0.06	23 ± 4	32 ± 2
3 mol%-PEG	130 ± 5	0.05 ± 0.01	23 ± 3	28 ± 2
7 mol%-PEG	126 ± 7	0.06 ± 0.01	21 ± 1	21 ± 5
12 mol%-PEG	130 ± 3	0.08 ± 0.01	13 ± 4	13 ± 3